Journal of Peptide Science
J. Peptide Sci. 2006; **12**: 51–57
Published online 9 June 2005 in Wiley InterScience (www.interscience.wiley.com). DOI: 10.1002/psc.687

JOURNAL OF PEPTIDE SCIENCE

Conformational analysis of human calcitonin in solution

KIYOSHI OGAWA,[a] SHIGENORI NISHIMURA,[b] MASAMITSU DOI,[a] HIROYUKI TAKASHIMA,[a] YOSHINORI NISHI,[a,c] TAKUYA YOSHIDA,[a] TADAYASU OHKUBO[a] and YUJI KOBAYASHI[a,c]*

[a] Graduate School of Pharmaceutical Sciences, Osaka University, Suita, Osaka, 565-0871 Japan
[b] College of Agriculture, Osaka Prefecture University, Sakai, Osaka, 599-8531 Japan
[c] Osaka University of Pharmaceutical Sciences, Takatsuki, Osaka, 569-1094, Japan

Received 11 February 2005; Accepted 18 February 2005

Abstract: The solution conformation of human calcitonin in a mixture of 60% water and 40% trifluoroethanol has been determined by the combined use of ^{1}H NMR spectroscopy and distance geometry calculations with a distributed computing technique. ^{1}H NMR spectroscopy provided 195 distance constraints and 13 hydrogen bond constraints. The 20 best converged structures exhibit atomic rmsd of 0.43 Å for the backbone atoms from the averaged coordinate position in the region of Asn^3 – Phe^{22}. The conformation is characterized by a nearly amphiphilic α-helix domain that extends from Leu^4 in the cyclic region to His^{20}. There are no significant differences observed among the overall structures of a series of calcitonins obtained from ultimobranchial bodies, including those that possess 20- to 50-fold greater activity. Three aromatic amino acid residues, Tyr^{12}, Phe^{16} and Phe^{19}, form a hydrophobic surface of human calcitonin. Bulky side chains on the surface could interfere with the ligand–receptor interaction thereby causing its low activity, relative to those of other species.

Keywords: calcitonin; human calcitonin; eel calcitonin; NMR; amphiphilic α-helix

INTRODUCTION

Calcitonin is an endogenous peptide which acts principally on bone as a regulator of calcium homeostasis. The peptide is produced and secreted by the parafollicular cells (C-cells) located in the thyroid glands of mammals and in the ultimobranchial bodies in non-mammalian vertebrates. The therapeutic use of calcitonin is to treat disorders in calcium metabolism involving hypocalcaemia, Paget's disease and osteoporosis. The physiology and pharmacology of calcitonin have been reviewed by Azria [1]. While the primary structures of calcitonins from various species differ, they do show the following common features: (i) a chain length of 32 amino acid residues, (ii) a disulfide bridge between two cysteine residues at position 1 and 7 in the *N*-terminal portion and (iii) a proline amide residue at the *C*-terminal end. The amino acid sequences of calcitonins mentioned in this work are listed in Figure 1.

Despite these common features, differences in the biological potencies of those various calcitonins have been reported. Those obtained from non-mammalian species generally have more potent biological activities than those of mammalian origin. For instance, the biological activity of human calcitonin (hCT) is about 50-fold weaker than that of salmon calcitonin (sCT) [2].

The relationship between structure and biological activity of calcitonins has attracted much interest. Using the Chou and Fasman method, Merle *et al.* predicted that the segment 4–20 of sCT should consist of α-helix, whereas there should be no helix but only β-sheets and turns in hCT. They also suggested that the helix forming potential could be correlated with the biological activity of calcitonin [3]. However, CD spectra have revealed that actually calcitonins, including sCT, have little ordered secondary structure in aqueous solutions. In the presence of phospholipids or trifluoroethanol [4,5], the CD spectra with a double trough indicate the formation of an α-helix. Furthermore, NMR studies on sCT in aqueous trifluoroethanol [6] and methanol [7] indicated the presence of an α-helical structure between residues 8–22. Motta *et al.* have reported that sCT [8] and hCT [9] in aqueous dimethylsulfoxide solutions, so-called cryomixtures, assume an extended conformation with only short double-stranded antiparallel β-sheet regions but with no evidence of regular helical segments even at temperatures down to −37 °C. However, the addition of sodium dodecyl sulfate (SDS) to aqueous sCT solutions led to a predominantly helical conformation between Thr^6-Tyr^{22} [10]. The conformation of hCT in SDS micelles has been also reported by Motta *et al.* [11]. Their results showed that hCT consists of an amphiphilic α-helix region between Leu^9 and Leu^{16}, a type-I β-turn in the Phe^{16} – Phe^{19} and an extended structure in the *C*-terminal part. They suggested that the type-I β-turn structure might stabilize the *C*-terminus part of the helix by acting as an end-cap.

Introducing the idea of a helical wheel, Moe and Kaiser pointed out that if calcitonin takes a helical conformation it should be in the region of

*Correspondence to: Dr Y. Kobayashi, Graduate School of Pharmaceutical Sciences, Osaka University, 1-6, Yamadaoka, Suita, Osaka, 565-0871, Japan; e-mail: yujik@protein.osaka-u.ac.jp

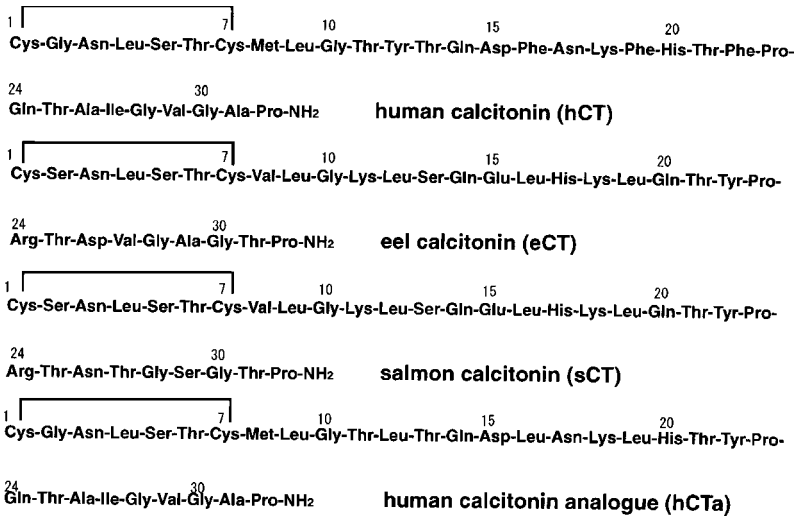

Figure 1 Primary structures of calcitonins.

residues 8–22, because the region 1–7 is incorporated in a cyclic moiety formed by a disulfide bond and Pro at position 23 terminating the proceeding helix. Consequently calcitonin should manifest an amphiphilic property, where the hydrophobic and hydrophilic side chains are segregated onto two faces of the helical cylinder [5]. They speculated that peptides bound to amphiphilic surfaces such as phospholipids, membranes and receptors tend to have binding sites comprising amphiphilic secondary structures. Therefore, it is reasonable to assume that an amphiphilic environment could impose a secondary structure on the peptide. This may be the reason why aqueous trifluoroethanol solutions are often employed to mimic *in vivo* amphiphilic environments.

The structure-activity relationship of calcitonins were studied mainly by substituting amino acids and/or by shortening the peptide chain of sCT [12–17]. The level of hypocalcaemic activity of the calcitonins is as follows: salmon calcitonin (sCT), eel calcitonin (eCT) > human calcitonin analogue (hCTa) mentioned below, > rat calcitonin > human calcitonin (hCT), porcine calcitonin. The synthetic calcitonin analogues, [Gly^{8}]sCT and [Ala^{16}]sCT, have higher biological activity than native sCT [18]. Their conformation had flexibility resulting from the substitution of amino acid residues with less bulky side chains and less tendency to take helical structures. Single deletion analogues, des-Leu^{16} sCT and des-Phe^{16} hCT, showed significant losses of biological activities. This indicated that the hydrophobicity of residue 16 in the calcitonin molecule is important for hormone binding [19]. In contrast to the number of studies of sCT, only a few studies using synthetic analogues of hCT have been reported. Maier *et al.* reported that an hCT analogue with Leu substitution at positions 12, 16 and 19 has a 10 fold greater activity compared with hCT [20]. Furthermore, Tyr substitution of this analogue at position 22 was shown to increase the activity 15–20 times. The previous studies had determined the trifluoroethanol solution structure of eCT [21] and hCT analogue (hCTa) in which substitutions of Leu^{12,16,19} and Tyr^{22} are incorporated in hCT [22] and proved the existence of an amphiphilic helix structure by the combined use of NMR experiments and distance geometry calculations. Although the solution conformation of hCT has been investigated by the same method, the resulting structures were of poor quality [23]. This study determined the conformation of hCT in an aqueous trifluoroethanol solution in order better to understand the low activity of hCT, and also to extend our understanding of the structure/activity relationships of calcitonin.

MATERIALS AND METHODS

Synthetic human calcitonin was a gift from Ciba-Geigy (Japan), and was used without further purification.

Sedimentation Equilibrium

The sedimentation equilibrium experiments were performed with a Beckman Optima XL-I analytical ultracentrifuge at 50 000 rpm at 25 °C. The human calcitonin was dissolved at a concentration of 2 mM in a mixture of 60% water and 40% trifluoroethanol containing 0.05 M acetic acid. An absorbance scan at 287 nm was measured in the radial step. The partial specific volume of human calcitonin (0.726 cm^3/g) was estimated from the amino acid composition by the method of Cohn and Edsall [24]. The molecular weight was determined by the sedimentation equilibrium method using the same method as described in a previous study [21].

NMR Experiments

The NMR samples were a 2.0 mM solution of hCT in 60% water and 40% (1-^{2}H$_2$)trifluoroethanol containing 0.05 M deuterated acetic acid. NMR measurements were performed at 600 MHz

on a Varian INOVA spectrometer and at 400 MHz on a Jeol LA-400 spectrometer, both at 5 °C and 30 °C.

A series of two-dimensional NMR spectra, double quantum filtered correlated spectroscopy (DQF-COSY) [25] and nuclear Overhauser enhancement spectroscopy (NOESY) [26,27], were recorded in the phase-sensitive mode using the methods of States *et al.* [28]. The water resonance was suppressed by low-power irradiation during the relaxation delay and mixing times. The relative exchange rates of the amide protons were investigated as follows. A dry sample of hCT was dissolved in 40% 2,2,2-trifluoroethanol-$^2H_3$/60% D_2O. A decrease in some of the amide proton peak intensities was observed in the one-dimensional spectra. After the rapidly exchanging peaks had disappeared, NOESY experiments were run to assign those remaining peaks. In order to obtain the inter-proton distances, NOESY spectra were recorded at various mixing times, i.e. 80, 100, 150 ms. The intensities of the NOE cross peaks in the NOESY spectrum were recorded with a mixing time of 80 ms and were translated to the inter-proton distances as reported in the previous work [21].

Structure Calculation

These distances were subjected as the distance constraints to the structure calculation which was carried out by distance geometry and simulated annealing calculations according to our recently developed procedure. This procedure employed a distributed computing technique to increase the number of initial structures to explore the conformational space comprehensively and to determine high resolution structures [29]. Initially, 4000–10 000 structures were generated from a random array, followed by 80 ps simulated annealing from a high initial temperature, 5000 K (Cartesian coordinates of all atoms were randomly varied from −10 Å to 10 Å. Randomness of the initial structures was verified by calculation of backbone rmsd value, 13.1 ± 0.3 Å). Then the final structures were selected by target energy. These calculations were performed using XPLOR-NIH v2.0 6 [30] on the distributed computing of 17 Linux PCs controlled by a SUN GRID engine.

RESULTS AND DISCUSSION

Aqueous trifluoroethanol, which has been widely used as a structure-inducing cosolvent, is known to stabilize the α-helical structure of peptides or protein fragment with an inherent helical propensity [31]. Peptides that reach their maximum helical content at much lower trifluoroethanol concentrations indicate that the inherent helical propensity of the sequence is high. In addition, there have been some observations of stable β-turn [32] and β-hairpin [33] structures in trifluoroethanol. Trifluoroethanol induces native-like structures in a peptide chain and stabilizes peptide helices or sheets in a sequence-dependent manner. Viguera *et al.* suggested that moderate amounts of trifluoroethanol can reveal a propensity for β-structure with α-spectrin [34]. This suggested that trifluoroethanol is not limited to promoting helix formation but also stabilizes β-structure. These facts indicated that trifluoroethanol distinguished between α- and β- structure induced by structural tendencies of the sequence. Therefore, trifluoroethanol does not always induce a helical conformation in any given peptide. This study used an aqueous trifluoroethanol mixture for the solvent as a mimic of *in vivo* amphiphilic environments following the previous experiments for eCT, an analogue of eCT: elcatonin, and an analogue of hCT: hCTa. [21,35,22]

Furthermore, the trifluoroethanol concentration dependence of the CD pattern (data not shown) for hCT demonstrates that hCT takes an α-helical conformation with the addition of trifluoroethanol and takes nearly random coil conformations in water. An isobestic point, indicating that a conformational transition occurs between two states, i.e. random coil and α-helical states, was found for hCT.

Although the fibrillation of hCT in aqueous solution is well known, Kanaori *et al.* investigated the fibrillation process of hCT by NMR and reported that there was no spectra change detected over 24 h at lower concentrations (1–20 mg/ml) in aqueous solution [36]. Here, the concentration dependence of NMR spectra of hCT was examined by one-dimensional ^{1}H-NMR measurements in the aqueous trifluoroethanol solution. There was no difference of chemical shift values and line widths in all spectra over the range of concentration 0.5–2 mM for a week. Furthermore, a sedimentation equilibrium measurement was carried out on the hCT solution to make sure that no intermolecular association occurred in the NMR sample solution. The apparent molecular weight distribution in a 2.0 mM solution of hCT is demonstrated by plotting the logarithms of the concentration versus the squares of the distance from the centre of rotors to a certain point in the centrifuge cell (Figure 2). It shows that they are obviously in a linear relation from the meniscus to the bottom. The increment of the straight line gives the apparent molecular weight to be 3200 which coincides with the molecular weight of hCT calculated from

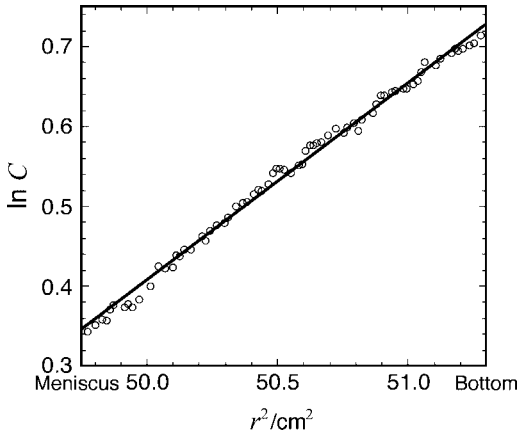

Figure 2 Plots of ln C versus $r^2 - a^2$ for the sedimentation equilibria of hCT in 60% water and 40% trifluoroethanol containing 0.05 M acetic acid at 25 °C.

its amino acid composition, 3417. This fact indicates that hCT exists in a mono disperse form without any association under these conditions which is same as that used in the NMR measurements.

The sequence specific assignments of proton resonances were made using standard procedures in NOESY and DQF-COSY spectra [37]. The finger print region of the NOESY spectrum is shown in Figure 3.

The profile of sequential NOE, $d_{\alpha N}$ and d_{NN}, and medium-range NOE, $d_{\alpha N}(i, i+3)$ and $d_{\alpha\beta}(i, i+3)$ connectivities along the polypeptide backbone, as well as the exchange rates of amide protons, are summarized in Figure 4. Cross peaks between protons on residues i and $i+3$, which are characteristic of an α-helical conformation, were observed in the region from Leu[4] to His[20]. Figure 5 displays the time-course of one-dimensional spectra of the amide proton region in the hydrogen-deuterium exchange experiment. The amide

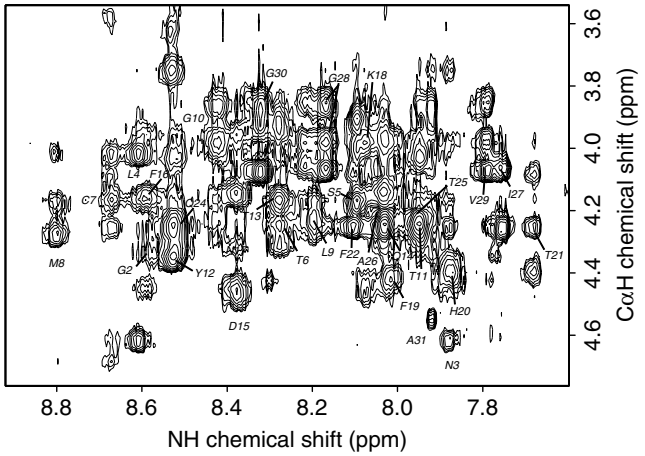

Figure 3 Fingerprint region of NOESY spectrum of hCT in 40% trifluoroethanol/60% water solution.

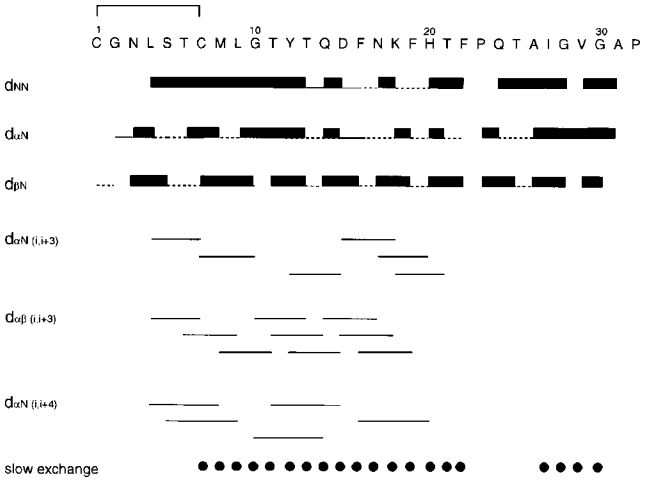

Figure 4 Summary of the NOE connectivities of the neighbouring residues. NOE intensities are indicated by the height of the bar. Terms d_{NN} and $d_{\beta N}$ represent the sequential backbone connectivities.

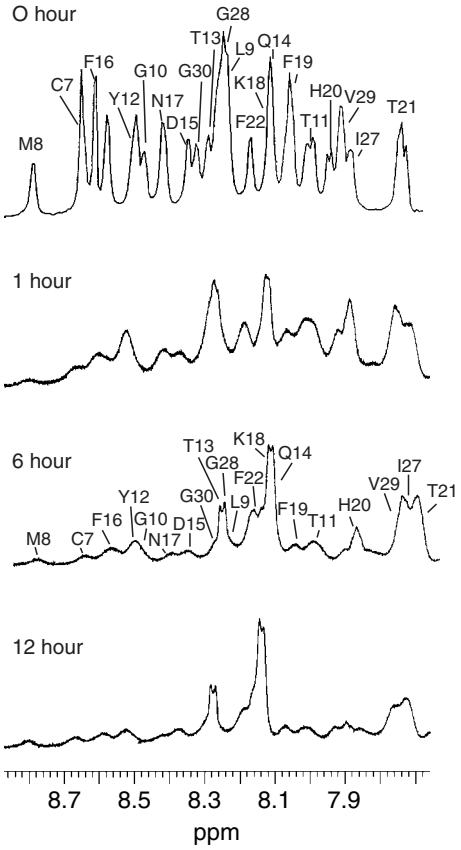

Figure 5 Time-course of the NH signals of hCT in hydrogen-deuterium exchange experiments.

protons of Met[8] – His[20] exchanged so slowly that they were still detected more than 12 h after dissolution. Thus the slowly exchanging protons listed in Figure 4 were assumed to be involved in hydrogen bonding and the position of the α-helix region was determined to be between Leu[4] and His[20].

Neglecting the NOEs detected between protons separated by less than three covalent bonds, because coherent magnetization might be mixed, a total of 195 NOEs were collected from the NOESY spectra with a mixing time of 80 ms and then converted into upper limit distance constraints for the structure calculations. Pseudo-atom treatments were applied for the methyl proton or methylene protons. The distance constraints on those pseudo-atoms were used during the calculations after multiplication by suitable correcting factors [38]. Stereospecific assignments for the β-methylene protons were established for nine residues by standard procedures using NH-CβH and CαH-CβH NOE contacts. The slowly exchanging amide protons, which were located in the previously identified helical region, were interpreted in terms of a CO(i) – N(i + 4) hydrogen bonds. A total of 13 hydrogen bond constraints were introduced into the structure calculations. The presence of a disulfide bond between Cys[1] and Cys[7] was fixed directly with distance

constraints. The 81 dihedral angle constraints of the amino acid residues were elucidated from the local structure analysis with the program HABAS [39].

Very recently, a new method was established for the high-resolution structure determination of bioactive peptides using a distributed computing implementation to calculate tens of thousands of structures to explore the conformational space [29]. This method was used on bioactive peptide endothelin-1 and thereby determined its *C*-terminal conformation, which was not evident in previous NMR studies. Given the success of this method, this procedure was employed to determine the high-resolution structure of hCT. First, the structure calculations were tentatively carried out with 195 distance constraints removing hydrogen bond constraints from the total 221 constraints. Starting from 4000 initial structures generated by random array, ten final structures with lowest energies of target function were selected. The average root-mean-square deviations (rmsd) of the backbone atoms for the region from Asn^3 to Phe^{22} was 1.1 ± 0.4 Å. The resulting structures, even though the information of hydrogen bonding was excluded, had a distinctly α-helical segment extending between Leu^4 and His^{20}. This region fits that where slowly exchanging protons were detected in the NMR experiment. This fact allowed us to incorporate the distance constraints relating hydrogen bonding that was assumed to stabilize helical structure in this region. Because the hydrogen bond constraints relating to α-helix have a tendency to determine the conformation predominately in the course of structure calculation, subjecting such constraints without preliminary checking might cause serious artefacts such as the formation of false helical structure.

Then in the next stage, structure calculations were carried out from 10 000 initial structures using hydrogen bond constraints by setting 2.0 ± 0.2 Å for HN-O and 3.0 ± 0.3 Å for N–O distances. These calculations yielded a total of 20 structures, which satisfied all distance constraints and consisted of lower target function. The resulting structure of hCT is characterized by an amphiphilic α-helical structure between Leu^4 and His^{20}, which spans into the cyclic moiety. The termination of the α-helical region in hCT is the His^{20} residue, which is not affected by a Pro^{23} residue. The region of $Thr^{21} - Phe^{22}$ allowed good convergence in these calculations, even though the characteristic medium-range NOE was not detected from the end of the α-helical structure. The resulting dihedral angles, $\phi(-81.9 \pm 0.9)$ and $\psi(-35.2 \pm 0.6)$ angles of Thr^{21} and $\phi(-144 \pm 0.7)$ angle of Phe^{22}, are within the permissible range of α-helical structure, but were not given a defined structure such as 3_{10}-helix.

The structures are superimposed in the $Cys^1 - His^{20}$ region by means of least squares fitting of the backbone atoms and are illustrated in Figure 6. They showed such good convergence that the mean rmsd values, among the 20 best structures from residue 3–22, decrease to 0.43 ± 0.18 Å for the backbone atoms. This good convergence for this size peptide obviously showed how well our new calculation procedure works. The side chains of amino acid residues in the α-helical region have a well-defined structure that clearly show aromatic ring stacking between the side chains of Tyr^{12} and Phe^{16}. This ring stacking contributes to the stability of α-helix. In contrast, the remaining peptide residues at the *C*-terminal side showed poor convergence. This lack of convergence reflects the absence of any structurally significant NOE restraints for the *C*-terminal region and no secondary structure was determined. However, it should be noted that the observation of medium-range NOEs at the *C*-terminus in NMR measurements might have been precluded by overlapping resonances.

The Structure/Activity Relationship of Calcitonin

The relationship between the ability to regulate calcium homeostasis and the potency to form a helical structure in calcitonin has been already pointed out [2]. Pioneering work by Kaiser and his colleagues revealed that the sequences of calcitonins between residues 8 and 22 have regularly spaced hydrophobic residues, indicating a possible propensity for amphiphilic α-helical structures [40]. They designed and synthesized a model peptide to show that the formation of amphiphilic helix is requisite and tried to demonstrate the correlation between activity and the steric properties of side chains of the helix. However it has been difficult to discuss the structure-activity relationship of the bioactive peptide without the reliable detailed information about its solution structure.

Now three structures of calcitonin from various sources, i.e. eCT [21], sCT [6] and hCT (this work), are available and also two structures have been determined for the analogues of hCT and eCT, named hCTa [22] and elcatonin [35] respectively. Furthermore, the relative biological activities among them are known, i.e. assuming the potency of therapy for hypercalcaemia of hCT as one, eCT and sCT are 40 [1] and hCTa is 15–20 [20]. The above information makes it possible to investigate the pending problem of structure-activity relationship of calcitonin in detail. The facts that hCT, eCT and hCTa take a helical structure between the residues 4–20 respectively and sCT takes it between residues 8 and 22 show that the relation between helical length and the biological activity is not straightforward even though such a simple correlation had been suggested.

The helical wheel projection in Figure 7A indicates that α-helical region between Leu^4 and His^{20} in hCT does not form a complete amphiphilic helical structure. Most of hydrophilic amino acid residues are located in the upper part of the helical wheel projection, while

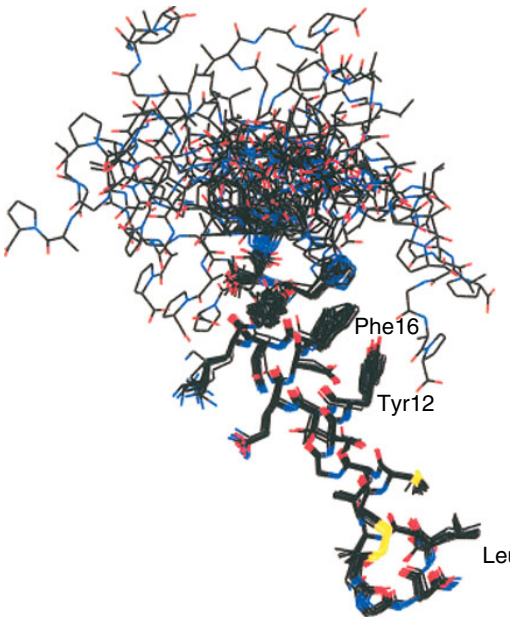

Figure 6 Overlay of 20 minimum energy structures of hCT, fitting residues 1 to 20.

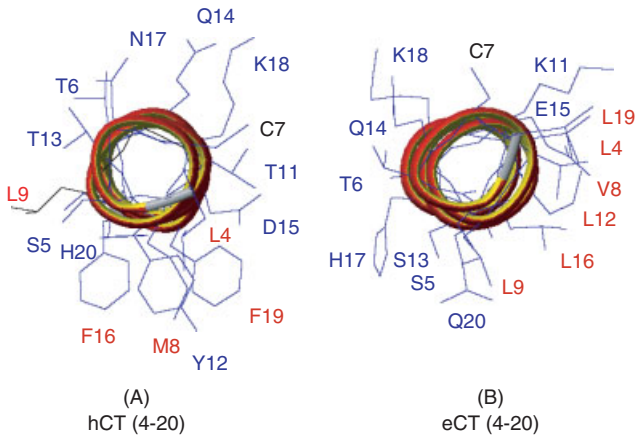

Figure 7 Helical wheel projection of hCT (A) and eCT (B) between residues 4 and 20.

hydrophobic amino acid residues are located in the lower part where some hydrophilic residues are mixed in. On the other hand for those which show potent activities, the projection in Figure 7B obviously shows that the α-helical region between Leu^4 and Gln^{20} in eCT forms an amphiphilic helical structure where one Val and five Leu residues, Leu^4, Val^8, Leu^9, Leu^{12}, Leu^{16} and Leu^{19}, form a complete hydrophobic surface and the remaining residues form an hydrophilic surface at the opposite side. The helical region of sCT, which has coincidently the same amino acid sequence to that of eCT, has the same spatial alignment. The fact that eCT and sCT, both of which show potent biological activity, form a complete hydrophobic surface indicates that such a well segregated amphiphilic helical formation is requisite for the high potent biological activity of calcitonin.

The lower part of helical wheel projection of hCT consists of aromatic side chains of Tyr^{12}, Phe^{16} and Phe^{19} in addition to those of Leu^4, Ser^5, Met^8, Leu^9 and His^{20}. These three aromatic side chains form a bulky core on the hydrophobic surface of hCT, which provides a different feature from those surfaces of eCT and sCT. Our previous work on hCTa that was synthesized by the substitutions of each of these hCT aromatic residues with Leu revealed that all the Leu side chains including that of the original Leu^9 forms a complete hydrophobic surface. The weaker activity of hCT compared with that of hCTa should be attributed to the difference between the features of their hydrophobic surfaces. It is likely that the bulky core of aromatic side chains interfere with the interaction between the ligand and its receptor in the case of hCT. The weaker activities of hCT and hCTa than those of eCT and sCT should be attributed to the degrees of segregation between the hydrophobic and hydrophilic residues. In the hydrophobic region of hCT and hCTa there are concomitant hydrophilic residues, i.e. Ser^5 and His^{20}.

CONCLUSIONS

In conclusion, the well separated amphiphilic helical structure with complete hydrophobic surface without aromatic side chains found in eCT and sCT, which may provide a suitable binding site to the receptor, produces the potent activity of calcitonin.

Supplementary Material

Solution structures of hCT and hCTa in the helical region (SM1) are available from the authors upon request.

Acknowledgements

We thank Dr Evelyn R. Stimson and Dr Vincent J. Huber for their helpful discussions.

REFERENCES

1. Azria M. *The Calcitonin; Physiology and Pharmacology*. Karger: Basel, 1989.
2. Guttman S. Chemistry and structure-activity relationship of natural and synthetic calcitonins. In *Calcitonin 1980: Chemistry, Physiology, Pharmacology, and Clinical Aspects*, Pecile A (ed.). Exerpta Medica: Princeton: NJ, 1980; 11–24.
3. Merle M, Lefevre G, Milhaud G. Predicted secondary structure of calcitonin in relation to the biological activity. *Biochem. Biophys. Res. Commun.* 1979; **87**: 455–460.
4. Epand RM, Epand RF, Orlowski RC, Schulueter RJ, Boni LT, Hui SW. Amphipathic helix and its relationship to the interaction of calcitonin with phospholipids. *Biochemistry* 1983; **22**: 5074–5084.
5. Moe GR, Miller RJ, Kaiser ET. Design of a peptide hormone: Synthesis and characterization of a model peptide with calcitonin-like activity. *J. Am. Chem. Soc.* 1983; **105**: 4100–4102.

6. Meyer JP, Pelton JT, Hoflack J, Saudek V. Solution structure of salmon calcitonin. *Biopolymers* 1991; **31**: 233–241.
7. Meadows RP, Nikonowicz EP, Jones CR, Bastian JW, Gorenstein DG. Two-dimensional NMR and structure determination of salmon calcitonin in methanol. *Biochemistry* 1991; **30**: 1247–1254.
8. Motta A, Morelli MAC, Goud N, Temussi PA. Sequential ^{1}H NMR assignment and secondary structure determination of salmon calcitonin in solution. *Biochemistry* 1989; **28**: 7996–8002.
9. Motta A, Temussi PA, Wunsch E, Bovermann G. A ^{1}H NMR study of human calcitonin in solution. *Biochemistry* 1991; **30**: 2364–2371.
10. Motta A, Pastore A, Goud NA, Morelli MAC. Solution conformation of salmon calcitonin in sodium dodecyl sulfate micelles as determined by two-dimensional NMR and distance geometry calculations. *Biochemistry* 1991; **30**: 10 444–10 450.
11. Motta A, Andreotti G, Amodeo P, Strazzullo G, Morelli MAC. Solution structure of human calcitonin in membrane-mimetic environment: The role of the amphiphilic helix. *Proteins* 1998; **32**: 314–323.
12. Schwartz KE, Orlowski RC, Marcus R. des-Ser^{2} salmon calcitonin: A biologically potent synthetic analog. *Endocrinology* 1981; **108**: 831–835.
13. Findlay DM, Michelangeli VP, Martin TJ, Orlowski RC, Seyler JK. Conformational requirements for activity of salmon calcitonin. *Endocrinology* 1985; **117**: 801–805.
14. Epand RM, Stahl G, Orlowski RC. Conformational and biological properties of partial sequences of salmon calcitonin. *Int. J. Peptide Protein Res.* 1986; **27**: 501–507.
15. Orlowski RC, Epand RM, Stanfford AR. Biological potent analogues of salmon calcitonin which do not contain an *N*-terminal disulfide-bridge ring structure. *Eur. J. Biochem.* 1987; **162**: 399–402.
16. Epand RM, Epand RF, Stafford AR, Orlowski RC. Deletion sequences of salmon calcitonin that retain the essential biological and conformational features of the intact molecule. *J. Med. Chem.* 1988; **31**: 1595–1598.
17. Yates AJ, Gutierrez GE, Garrett IR, Mencel JJ, Nuss GW, Schreiber AB, Mundy GR. A noncyclical analog of salmon calcitonin (N^{α}-propionyl di-Ala^{1,7}, des-Leu^{19} sCT) retains full potency without inducing anorexia in rats. *Endocrinology* 1990; **126**: 2845–2848.
18. Epand RM, Epand RF. Conformational flexibility and biological activity of salmon calcitonin. *Biochemistry* 1986; **25**: 1964–1968.
19. Findlay DM, Michelangeli VP, Orlowski RC, Martin TJ. Biological activities and receptor interactions of des-Leu^{16} salmon and des-Phe^{16} human calcitonin. *Endocrinology* 1983; **112**: 1288–1291.
20. Maier R, Kamber B, Rinker B, Pittel W. Analogues of human calcitonin. *Clin. Endocrinol.* 1976; **5**: 327–332.
21. Ogawa K, Nishimura S, Uchiyama S, Kobayashi K, Kyogoku Y, Hayashi M, Kobayashi Y. Conformation analysis of eel calcitonin. Comparison with the conformation of elcatonin. *Eur. J. Biochem.* 1998; **257**: 331–336.
22. Katahira R, Doi M, Kyogoku Y, Nosaka-Yamada A, Yamasaki K, Takai M, Kobayashi Y. Solution structure of a human calcitonin analog elucidated by NMR and distance geometry calculations. *Int. J. Peptide Protein Res.* 1995; **45**: 305–311.
23. Doi M, Kobayashi Y, Kyogoku Y, Gohda K, Takimoto M. Structure study of human calcitonin. *Proceeding of the 11th American Peptide Symposium*, River JE, Marshall GR (eds). ESCOM; Leiden, 1989; 165–167.
24. Cohn EJ, Edsall JT. *Proteins, Amino Acids and Peptides as Ions and Dipolar Ions*. Reinhold: New York, 1943.
25. Rance M, Sorensen OW, Bondenhausen G, Wagner G, Ernst RR, Wüthrich K. Improved spectral resolution in COSY ^{1}H NMR spectra of proteins via double quantum filtering. *Biochem. Biophys. Res. Commun.* 1983; **117**: 479–485.
26. Jeener J, Meier BH, Bachmann P, Ernst RR. Investigation of exchange processes by two-dimensional NMR spectroscopy. *J. Chem. Phys.* 1979; **71**: 4546–4553.
27. Kumar A, Ernst RR, Wüthrich K. A two-dimensional nuclear Overhauser enhancement (2D NOE), experiment for the elucidation of complete proton-proton cross-relaxation networks in biological macromolecules. *Biochem. Biophys. Res. Commun.* 1980; **95**: 1–6.
28. States DJ, Haberkorn RA, Ruben DJ. A two-dimensional nuclear Overhauser experiment with pure absorption phase in four quadrants. *J. Magn. Reson.* 1982; **48**: 286–292.
29. Takashima H, Mimura N, Ohkubo T, Yoshida T, Tamaoki H, Kobayashi Y. Distributed computing and NMR constraint-based high-resolution structure determination: Applied for bioactive peptide endothelin-1 to determine *C*-terminal folding. *J. Am. Chem. Soc.* 2004; **126**: 4504–4505.
30. Schwieters CD, Kuszewski JJ, Tjandra N, Clore GM. The Xplor-NIH NMR molecular structure determination package. *J. Magn. Res.* 2003; **160**: 65–73.
31. Sonnichsen FD, Van Eyk JE, Hodges RS, Sykes BD. Effect of trifluoroethanol on protein secondary structure: An NMR and CD study using a synthetic actin peptide. *Biochemistry* 1992; **31**: 8790–8798.
32. Siligardi G, Drake AF, Mascagni P, Neri P, Lozzi L, Niccolai N, Gibbons WA. Resolution of conformational equilibria in linear peptides by circular dichroism in cryogenic solvents. *Biochem. Biophys. Res. Commun.* 1987; **143**: 1005–1011.
33. Blanco FJ, Jimenez MA, Pineda A, Rico N, Santori J, Nieto JL. NMR solution structure of the isolated *N*-terminal fragment of protein-G B1 domain. Evidence of trifluoroethanol induced native-like β-hairpin formation. *Biochemistry* 1994; **33**: 6004–6014.
34. Viguera AR, Jimenez MA, Rico M, Serrano L. Conformational analysis of peptides corresponding to β-hairpins and a β-sheet that represent the entire sequence of the α-spectrin SH3 domain. *J. Mol. Biol.* 1996; **255**: 507–521.
35. Ogawa K, Nishimura S, Doi M, Kyogoku Y, Hayashi M, Kobayashi Y. Conformational analysis of elcatonin in solution. *Eur. J. Biochem.* 1994; **222**: 659–666.
36. Kanaori K, Nosaka YA. Study of human calcitonin fibrillation by proton nuclear magnetic resonance spectroscopy. *Biochemistry* 1995; **34**: 12 138–12 143–.
37. Wüthrich K. *NMR of Proteins and Nucleic Acids*. John Wiley: New York, 1986.
38. Wüthrich K, Billeter M, Braun W. Pseudo-structure for the 20 common amino acids for use in studies of protein conformations by measurements of intramolecular proton-proton distance constraints with nuclear magnetic resonance. *J. Mol. Biol.* 1983; **169**: 949–961.
39. Guntert P, Braun W, Billeter M, Wüthrich K. Automated stereospecific ^{1}H NMR assignments and their impact on the precision of protein structure determinations in solution. *J. Am. Chem. Soc.* 1989; **111**: 3997–4004.
40. Moe GR, Kaiser ET. Design, synthesis and characterization of a model peptide having potent calcitonin-like biological activity; Implication for calcitonin structure/activity. *Biochemistry* 1985; **24**: 1971–1976.